# Local disorder in lithium imide from density functional simulation and NMR spectroscopy

Bonnet, Marie-Laure ; Iannuzzi, Marcella ; Sebastiani, Daniel ; Hutter, Jürg

Abstract: Born–Oppenheimer molecular dynamics simulations in combination with calculations of 1H, 7Li, and 15N NMR chemical shifts are used to characterize lithium imide structures at different temperatures. Indications of the onset of local disorder in the lithium sublattice, leading eventually to superionicity, are recognized already at low temperature (100 K). Between 100 and 400 K, a new structure could be stabilized, which presents features that are intermediate between the previously reported Fm3m and the Fd3m structures. The disorder in the Li positions is associated with the reorientation of the NH bonds, which preferentially point toward Li-vacant sites. Clear signatures of such structural rearrangements are visible in the simulated NMR spectra, where smoother profiles are associated with a reduced amount of Li interstitials and a higher occupation probability of the antifluorite sites.

DOI: https://doi.org/10.1021/jp3004272

# Local Disorder in Lithium Imide from density functional simulation and NMR Spectroscopy

*Marie-Laure Bonnet,[a] Marcella Iannuzzi,*[a] Daniel Sebastiani,[b] and Jürg Hutter[a]*

[a] Physikalisch-chemisches Institut, Universität Zürich

Winterthurerstrasse 190, 8057 Zürich (Switzerland)

Fax: (+41)44-635-6838

[b] Dahlem Center for Complex Quantum Systems

Institute for Theoretical Physics, Freie Universität Berlin

Arnimallee 14, 14195 Berlin (Germany)

AUTHOR EMAIL ADDRESS marcella@pci.uzh.ch

**RECEIVED DATE (to be automatically inserted after your manuscript is accepted if required according to the journal that you are submitting your paper to)**

ABSTRACT

Born-Oppenheimer Molecular Dynamics Simulations in combination with calculations of $^{1}H$, $^{7}Li$, and $^{15}N$ NMR chemical shifts are used to characterize Lithium Imide structures at different temperatures. Indications of the onset of local disorder in the Lithium sublattice, leading eventually to superionicity, are recognized already at low temperature (100K). Between 100K and 400K, a new structure could be stabilized, which presents features that are intermediate between the previously reported Fm-3m and the

Fd-3m structures. The disorder in the Li positions is associated with the re-orientation of the NH bonds, which preferentially point toward Li-vacant sites. Clear signatures of such structural rearrangements are visible in the simulated NMR spectra, where smoother profiles are associated with a reduced amount of Li interstitials and a higher occupation probability of the antifluorite sites.

KEYWORDS

Hydrogen storage compounds, *Ab initio* molecular dynamics simulation, Solid-state NMR spectroscopy

BRIEFS

The structural picture of Lithium Imide compounds is critically revised on the atomic scale. The local conformation of this system is crucial for understanding their microscopic hydrogen uptake and release processes.

MANUSCRIPT TEXT

## Introduction

The decreasing availability and increasing (energetic) mining costs of fossil fuels will soon impose a shift in the type of primary energy sources and energy carriers on which our society relies. In particular, we must find a technologically suitable way to sustain mobility and transportation. Hydrogen ($H_2$) as a fuel is considered one of the most promising energy carriers for vehicles and can potentially achieve zero $CO_2$ emission. The most convenient method to store and transport hydrogen is to stock $H_2$ by means of physisorption or chemisorption[1] into solid-state host structures. The selection of a good ratio between cargo load and host structure weight is economically of critical importance. One of the most promising, lightweight hydrogen storage system involves the hydrogen cycling between lithium nitride, lithium imide, and lithium amide, which is supposed to occur by the activation of the following reaction processes.[2]

$Li_3N + H_2 \rightarrow Li_2NH + LiH$ (I)

$Li_2NH + H_2 \rightarrow LiNH_2 + LiH$ (II)

The reactions (I) and (II) are expected to provide a storage potential of 10.4 wt%. However, the complete desorption of $H_2$ (I) requires temperatures higher than 320ºC (≈600K) in high vacuum ($10^{-5}$ mbar)[2a]. On the other hand, the alkali imide/amide transformation is an interesting process, due to the high storage density (6.5%) of $LiNH_2$, which can be exploited through the inverse of process (II) (desorption of $H_2$). The knowledge of the $Li_3N$ based storage is still considered of value for the development of solid state storage materials in the future. Several experimental and theoretical studies in gas phase have been carried out in the past years in order to understand the processes involving LiH, $LiNH_2$, and $Li_2NH$ and to assign the correct kinetics and reactivities[3]. However, processes involving solid state mixtures and the role of diffusion of H and Li in bulk and at the interfaces are still not fully understood. In particular, while the crystallographic structures of LiH and $LiNH_2$ are well established, $Li_2NH$ turned out to be a rather complex system, for which the local arrangement of Li and H atoms is still a matter of debate. It has been reported that the material undergoes an order-disorder transition at around 360K[4]. However, there is still no general consensus on the structures of the low and high temperature phases.[5,6] Recent results seem to indicate that the low temperature crystal structure of lithium imide has the Fd-3m space group symmetry, with lattice constant of 10.1 Å. This structure can be seen as a reconstruction of the antifluorite lattice. Indeed, the $NH^{2-}$ ions occupy the fcc sublattice, and the N atoms are tetrahedral coordinated to Li atoms on antifluorite sites. However, these latter sites are only partially occupied, since the Li atoms tend to occupy interstitial sites. The resulting structure has a larger unit cell and lower symmetry if compared to the antifluorite lattice (Fm-3m).[6] The order-disorder transition occurring at 360K involves displacements of Li atoms and the reorientation of NH groups. Neutron diffraction measurements confirmed the antifluorite structure for the high temperature phase of $Li_2NH$.[6] Several attempts have been made to identify the equilibrium distribution of Li interstitials and vacancies of the low temperature phase by means of first principle calculations.[6-7] It turned out to be quite difficult to build a simple model that satisfies the Fd-3m symmetry and could be stabilized at finite

temperature. More recently, two new structures have been proposed, based on the observation of the instability of the perfect antifluorite structure of Li ions along first principles molecular dynamics simulations at 300K. Luduena *et al.*[8] propose a revised structure characterized by pronounced disorder of the lithium sublattice. Such local disorder, which cannot be detected in X-ray and neutron diffraction, is consistent with the high diffusivity of Li, eventually leading to the known phase transformation and the superionic behaviour. From now on we denote this structure as Fd-3m A. Also the structure proposed by Miceli *et al.*[9] comes from a close inspection of molecular dynamics trajectories which proposed still a pronounced disorder of the Li sublattice with spontaneous formation of Frenkel pairs. They observed that interstitial Li atoms might form tetrahedral clusters with a Li2 vacancy at their center. These clusters stabilize the structure by preventing further diffusion of Li interstitials. The smallest supercell consistent with the stoichiometry consists of 192 atoms and contains 4 vacancy-interstitials clusters evenly distributed, to balance the negatively charged constitutional vacancies. We call this structure Fd-3m B.

The atomistic structural parameter that discriminate among the locally disordered Fm-3m structure and the two newly proposed structures, (Fd-3m A) and (Fd-3m B), are not directly accessible by experimental techniques. In this material the local disorder of the light element Li and H has a crucial role in stabilizing the structure. In this case it is difficult to resolve the structural details, in particular the local environment of defects, with global crystallographic probes like the X-ray diffraction. From the diffraction pattern the two Fd-3m structures can be discriminated only from subtle changes. On the other hand, nuclear magnetic resonance (NMR) spectroscopy can provide a more detailed insight into the local environment. In this work, the characterization of the atomic structure of $Li_2NH$, as obtained from geometry optimization or by molecular dynamics equilibration at different temperatures, is combined with the calculation of H, Li, and N NMR chemical shifts. The goal is to identify signatures in the NMR spectra that can be associated with specific features of the local environment and can be used to discriminate among the possible structures. The comparison to solid-state NMR experiments, when available, could then be used to support or invalidate given structural propositions. To this purpose, we

first consider the results of the optimizations starting from the three structures discussed in previous works, i.e. the ideal Fm-3m lattice, and the defective structures (Fd-3m A) and (Fd-3m B). These structures differ for the arrangements of Li interstitials and vacancies. Therefore, we look for signatures of these structural differences and in their NMR spectra. In the second part of the discussion, the effects of equilibration at finite temperature are considered by running first principles molecular dynamics starting from the defective (Fd-3m A) structure. The diffusion of the Li atoms occurs by hopping between interstitial sites and antifluorite lattice sites, and at higher temperatures this leads to a statistical distribution of the Li atoms closer to the higher symmetry group Fm-3m. We discuss the possibility to recognize this transformation from NMR spectroscopy.

## Computational Methods

The starting atomic configurations employed in this study are the (2x2x2) ideal antifluorite structure with lattice constant of 5.007 Å and 128 atoms in total, the optimized coordinates of (Fd-3m A, 128 atoms), as provided in Ref.[8], and the averaged coordinates of (Fd-3m B, 192 atoms), as provided in Ref.[9]. For the geometry optimizations and for MD runs at lower temperatures (100K and 300K), larger simulation cells have been used in order to take into account possible size effects on the rearrangement of defects. Simulation cells consisting of 1024 atoms, corresponding to 2x2x2 replicas of the smaller ones, have been used for Fm-3m and (Fd-3m A), while a simulation cell consisting of 768 atoms, 1x2x2 replicas of the smaller one, has been used for (Fd-3m B).

All calculations have been performed with the CP2K program package[10] and are based on density functional theory[11] in the generalized gradient approximation using the BLYP exchange-correlation functional.[12] For standard simulations the hybrid Gaussian and plane wave (GPW) formalism is employed together with the pseudopotential approximation, in order to describe the interaction between valence electrons and ionic cores. Goedecker-Teter-Hutter pseutopotentials[13] and double-zeta MOLOPT basis sets (DZVP-MOLOPT-SR-GTH)[14] are used for all elements. For the expansion of the charge density in plane waves, an energy cut-off of 300 Ry is used. In such crowded materials, with

high coordination numbers for all the species, dispersion contributions might become important. Therefore, empirical van der Waals corrections are always applied, following the DFT-D2 scheme proposed by Grimme.[15] The simulations at constant temperatures, ranging from 100K to 900K, have been performed starting from the optimized structure of (Fd-3m A) and using a time step of 1fs. The equilibration procedure at each considered temperature involves the generation of trajectories of 60ps, of which the first 15ps are carried out in the canonical ensemble (NVT), by controlling the temperature by means of a thermostat, the next 15ps are performed without the thermostat to check whether the equilibrium temperature is maintained and the total energy is conserved, and the final 30ps are in the microcanonical ensemble (NVE) and are used for the analysis. Radial and angular distribution functions are obtained by sampling the structure over the last 20ps. Average coordinates over the same time span are extracted in order to identify possible structural motifs and to simulate the X-ray diffraction spectra. For the sake of comparison, the same equilibration procedure has been applied for LiH and $LiNH_2$ at room temperature. Namely, crystallographic positions and NMR spectra of these materials are well established,[16,17] and their simulation can be useful as validation of the computational set up.[8] All NMR calculations are based on the all-electron version of the Gaussian and augmented-plane-wave (GAPW) method as implemented in CP2K.[18] The present approach to compute the induced current density generated by the magnetic field and, consequently, the shielding tensors and the magnetic susceptibility, is described in details in Ref. [19]. The standard all electron cc-pVTZ basis set[20] is employed for N atoms, while for Li and H the basis sets have been optimized ad-hoc to get the best performance within the GAPW scheme.[21] To be able to compare our results to experimental values, only the isotropic component of the tensor is considered and the chemical shift is computed taking as reference the TMS molecule for H, LiCl solvated in water for Li, and $CH_3NO_2$ for N (see supporting information). The simulated NMR spectra at finite temperature are computed by averaging over a set of snapshots extracted from the MD trajectory at every of 0.1ps. The sampling set of about 200 configurations is taken from the last 20ps of the NVE trajectory and the NMR simulation is performed for each of them. The quality of this sampling procedure is confirmed by the good convergence of the shielding

associated to individual atoms and by the lack of correlation among consecutive spectra (see supporting information).

## Results and Discussion

### Characterization of $Li_2NH$ optimized structures

Structure optimizations have been carried out for the three investigated structures. The starting configurations are the ideal 2x2x2 antifluorite lattice for Fm-3m, the structure reported in Ref. [8], replicated 2x2x2 times, for (Fd-3m A), (for the atomics positions see supporting information) and the structure reported in Ref. [9], replicated 1x2x2 times, for (Fd-3m B). After a geometry optimization at 0K, all the three structures appear to be stable and only slight deviations from the initial configurations are observed. The structural motifs characterizing the three geometries are reported in the supporting information. The H atoms are not reported in these sketches.

The highly ordered arrangement of Fm-3m, with all NH groups collinear with the z-axis, is found to be a local minimum at 0K, due to symmetry. However, as soon as some deviations from these ideal positions is introduced, for example by thermal fluctuations, the structure becomes unstable and Frenkel pairs are formed. In the other two structures, the distribution of Li-vacant antifluorite sites and interstitials determines the local orientation of the NH groups. In general the H atoms are oriented away from the Li interstitials and toward the vacancy, in order to compensate the missing positive charge. In (Fd-3m A) only half of the Li atoms occupy antifluorite sites, while the others are located in 96g sites (Li2). In the case of (Fd-3m B), the distribution of vacancies and interstitials is more complex, since some N-fcc units contain all the 8 Li atoms in antifluorite sites, some contain one or two vacant antifluorite site, and some contain the tetrahedral Li-interstitial cluster coordinating a Li-vacancy. The presence of defects introduces some distortion of the N sublattice, as it can be observed from the broader band of first neighbours in the N-N pair correlation function reported in Fig. 1. This distortion is more pronounced in the (Fd-3m B) due to the presence of the tetrahedral interstitial clusters. The lower

degree of local order of the two defective structures becomes evident from the Li-Li and the Li-N pair correlation functions. New features appear, with respect to the optimized antifluorite structure, between 3 Å and 4 Å, which are related to the presence of interstitial Li atoms in the first neighbour shells. At longer range, the variety of occupied Li sites and the lattice distortion are responsible for an almost even distribution of Li-N and Li-Li distances. The loss of symmetry going from Fm-3m to Fd-3m is also evident in the simulated X-ray diffraction patterns (Fig. 2). The intensities appearing below 20 degrees indicate a reduced size of the Brillouine zone, i.e larger lattice constant and the increased number of formula units per unit cell. These features are in agreement with experimental data.[6] On the other hand, the least ordered structure (Fd-3m B) turns out to be the lowest in energy, being 0.05 eV per formula unit more stable than (Fd-3m A), and 0.3 eV more stable than Fm-3m. Fm-3m is also the least dense structure, with an optimized volume per unit of 32.02 $Å^3$, while the volume per unit of (Fd-3m A) is 29.74 $Å^3$, and for (Fd-3m B) is 30.62 $Å^3$.

The NMR spectra computed on the three optimized structures at 0K are displayed in Fig. 3. The top panels report the Li (left), H (middle), and N (right) spectra obtained from the highly symmetric Fm-3m structure. In this case, each element is occupying only one type of site. The corresponding spectra show one localized feature, which indicates that the local environment for each element is basically equivalent over the whole simulation cell. In turn, the considerably broader distribution of the NMR chemical shift values for the (Fd-3m A) structure (center of Fig. 3) reveals strong variations in the local environment of all nuclei. The profile of the $^7$Li NMR spectrum shows three distinguished bands. The first above 4.4 ppm is the signal of those Li atoms in interstitial 96g position (ratio 4/8) (Fig. 3). The other two, at 3.3 ppm and 2.7 ppm, correspond to Li atoms occupying antifluorite sites, but experiencing different environments due to the distribution of vacancies and interstitials. The H and N spectra present still a single band, but displaced by a few ppm, with respect to the Fm-3m spectra, and broader, thus indicating some variations in the local environment of H and N as-well. The number of possible different environment characterizing the (Fd-3m B) structure is even larger, which is immediately recognized by the broad range over which the NMR signals are distributed. The spread of the spectral

profile does not only involve the Li spectrum, but also the H and N spectra, revealing a quite strong effect due to the lattice distortion and local distribution of vacancies and interstitials.

As already discussed in previous works, Frenkel pairs may spontaneously form in $Li_2NH$, which opens a multitude of possible locations for the corresponding interstitials. Common theoretical and experimental tools like pair correlation functions and X-ray diffraction patterns cannot reliably discriminate between different types of defective structures, falsely suggesting that the two are substantially equivalent. In contrast to this, the computed NMR spectra are substantially different, due to the high sensitivity of the chemical shift to the local environment.

## Equilibration of $Li_2NH$ at finite temperature

By increasing the temperature, the mobility of the Li ions is enhanced and the on-set of superionicity has also been hypothesized.[23;24] Thermal fluctuations at low temperature are already sufficient to destabilize the Fm-3m model in favor of the formation of a defective structure with Li Frenkel pairs. This has been observed also in previous MD studies.[9; 23, 25] The Li hopping events are associated with the rotation of the neighbouring NH groups. Also at finite temperature, several defects' distribution can be stabilized, where further hopping events of the interstitial Li atoms are quite rare. However, it is expected that, by increasing the temperature, the mobility of the Li atoms is further enhanced, leading to shorter life time of individual interstitials and an increased occupation probability of the antifluorite sites. Recent MD simulations starting from (Fd-3m B) show that above 500 K the tetrahedral clusters of interstitials dissolve and the Li interstitials start diffusing.[25]

In this work, we follow the time evolution of the (Fd-3m A) structure at finite temperature by running MD simulations. A wide range of temperatures has been considered, from 100 K to 900 K. The atomic positions describing the equilibrated structure at 300K are reported in table1, together with the partial occupation of specific crystallographic sites. The first observation is that the N sublattice is not significantly modified also at the highest tested temperatures. On the other hand, Li hopping events and changes in the orientation of the NH groups are observed already at low temperature and become more

frequent at higher temperatures. In particular, during the equilibration part of the trajectory, the Li interstitials, which are originally located at the 96g sites, are re-distributed. Most of them (~60%) move back to the vacant antifluorite sites, the others hop into interstitial sites of 4b type (Li3), which are found between N atoms along the [100] axis. The displacement of Li interstitials is also associated with the reorientation of the NH groups. Since after the relaxation the number of Li-vacancies is reduced, more H atoms, from 3 to 4, point to the same vacant site. The change in the nature of the interstitials is also indicated by some modifications in the Li-Li and Li-N pair correlation functions. By comparing the results obtained for the optimized structure (Fig. 1 middle panels) to the distribution averaged over the trajectory at 100 K and at 300 K (Fig. 4 top and middle panels), beside the general smoothening and broadening of the bands due to the thermal fluctuations, it is observed that the features at 3 Å disappear. Those peaks in the Li-Li and in the Li-N distributions at 0 K correspond to the Li2-Li2 and to the second neighbour Li2-N distances, respectively. At 100 K and 300 K, the pronounced Li-Li peaks at 3.5 Å and 4.2 Å, and the Li-N peak at 4 Å are features indicating a stable lattice close to the antifluorite structure. On the other hand, the first neighbour shells show tails towards larger distances due to the presence of the interstitials. Overall the radial distribution functions obtained at 100K and 300K look more similar to the one computed for the optimized (Fd-3m B) structure. This similarity is also revealed by the X-ray diffraction patterns (see supporting information), where the characteristic feature at 15 degrees appears, and the signal at 52 degrees becomes more pronounced. This new configuration is quite stable and Li hopping events are no longer observed along the trajectories generated below 400 K. This is also verified by the analysis of the mean square displacement, as computed over the last 20 ps at 100 K and 300 K, and reported in Fig. 4(c) (100K in blue, 300 K in green). Also the orientation of the NH group remains substantially the same, with the azimuthal angle distributed between two values, 55 and 125 degrees, conferring an antiferroelectric character to the NH sublattice. A sketch of the structure is proposed in Fig. 5 (a), where the averaged positions of Li and N atoms are reported.

We also find the interstitial Li atoms (Frenkel-pair) on 32e position. However, at 300K our rate is 0.344 instead of 0.26, as reported from experiment in the Ref. 6 for the Fd-3m at low temperature. We

have the full occupation for the 8a position too, but we have 8b full and not 48f in contrast to what previously reported. Concerning the H atoms, we report occupation of 96g sites instead of 32e. This can be an effect of the more regular arrangement of the N atoms, at 16c and 16d sites. In comparison to the experimental Ima2 structure, reported in the Ref. 7, the average nearest-neighbour distances in our 300K structure are larger, i.e. 2.1 vs 1.960Å for Li-N and 2.5 vs 2.218Å for Li-Li (see Fig. 4). On the other hand, the unit cell volume is smaller, 29.74 Å$^3$ vs, 31.76Å$^3$. These differences can also be related to the larger number of Li interstitials observed in our structure.

The tetrahedral interstitial arrangement with Li in 32e position with an antifluorite Li inside the tetrahedron is observed after MD equilibration at finite temperature. This feature is observed inside a primary cell (a=5.007 Å), while for Fd-3m B the tetrahedral arrangement it is observed between two primary cells. While in the optimized geometry Fd-3m A, the tetrahedral structure with the Li in 96g position contains no antifluorite Li, after MD equilibration, some Li interstitials are displaced to 32e position and, indeed, one Li occupies an antifluorite site within the tetrahedron formed by these interstitials. The distance between the interstitial Li (32e) atoms is approximately 3.5 Å. The resulting atomic arrangement reproduces some features of the Fd-3m B structure. However, the distance between separating the interstitial Li is about 1Å larger. Since several Li interstitials move to antifluorite sites by equilibration at 300K, the tetrahedral arrangement is not dominant; we observe only one such arrangement in the simulation box of size a=10.014Å. Moreover, the NH groups are oriented pointing to Li antifluorite vacancies and are arranged in antiferroelectric order (see supporting information on azimutal angle), thus compensating the positively charged region of tetrahedral interstitials. We observe similar tetrahedral groups of interstitials in the 1024 atoms box, even though less frequently. This is an indication that the formation of these groups is not a box-size effect.

At higher temperatures, e.g. at 600K, the number of Li interstitials is further reduced, being, on average, only one interstitial every 8 Li atoms. However, the number of atoms residing at least for some time in interstitial positions increases. This happens because the hopping events become more frequent and involve also atoms that already occupy antifluorite sites, hence promoting the overall mobility. The

pair distribution functions at higher temperature present broader bands that merge together, so that it is difficult to identify clear structural signatures. The enhanced mobility of the Li atoms is indicated by the constant increase of the Li MSD, as shown in the top panel of Fig. 4(c). Each site change of one Li atom is generally associated with the reorientation of some neighbouring NH groups. Such correlation appears also in the MSD of the H atoms that shows larger fluctuations when a hopping event occurs. However, the H atoms do not diffuse. On the other hand, the N sublattice is only slightly perturbed by these events, and the MSD of N atoms is still negligible. Indeed, over the last 20ps of the trajectory generated at 600 K, five Li hopping events are observed. By averaging the coordinates over the same time frame (Fig. 5 (b)), some Li atoms appear to be in intermediate position between lattice sites and interstitial sites. These results indicate that at higher temperature the structure has on average the antifluorite symmetry. The Li-antifluorite sites acquire a higher occupation probability, even though the instantaneous configurations are still defective. However, our MD simulations are too short to collect enough statistics to have a final averaged structure that is perfectly antifluorite.

## Simulated $^{1}$H, $^{7}$Li and $^{15}$N NMR chemical shift spectra at finite temperature

The effect of the Li mobility on the NMR spectra can be investigated by sampling the chemical shielding over the trajectories generated at different temperatures. LiH and $LiNH_2$ are compounds related to the imide, also playing an important role in the hydrogen cycling process mentioned in the introduction. The hydride and the amide structures are well established and several studies based on NMR techniques are available. In general, for ordered solid state systems, the average chemical shift for each addressed element is given. In Table 2, we compare the experimental average shift for Li and H in the three Li-H compounds, as reported in Ref. [25], to the values obtained by sampling over MD trajectories at 300 K. The standard deviations reported next to the computed averages refer to the sensitivity of the computed instantaneous NMR chemical shifts to structural fluctuations along the trajectory. The differences with respect to the experimental data are about 0.5 ppm, except for the Li shift in LiH, where the discrepancy to experiment is larger.

We note that the LiH sample used in the reported experiment was prepared from $LiNH_2$ by milling and heating near the temperature of reaction (II).[27] Other similar experimental studies[26,28] show spectra with two peaks for a mixture of $LiNH_2$ + LiH, one at around 2.7 ppm and the other around 1.9 ppm, where the 2.7 ppm signal is always assigned to $LiNH_2$. According to our results, it is reasonable to conclude that the peak at 1.9 ppm is the signature of crystalline LiH, and that, in the experiment reported in Ref. [26], the two contributions, from LiH and from $LiNH_2$, are still present.

In spite of the good agreement with experiment, the average shift value cannot fully reveal important details related to variations in the local environment and to the presence of defects. In order to better understand how structural changes and, in particular, the nature and distribution of Li interstitials can affect the spectra, we investigate the details of the spectral profiles at different temperatures. The spectra computed at 100K, 300K, and 600K are reported in Fig. 6. We observe that at 100K, and in part also at 300K (top and middle panels of Fig 6), the Li and the N spectra show structured profiles. The reason is that both elements experience different local environments due to the presence of Li Frenkel pairs. After equilibration at low temperature, the number of interstitials is reduced with respect to the optimized (Fd-3m A) structure, being 11/68 instead of 4/8. Hence, the larger contribution in the Li spectrum, at about 4 ppm, is attributed to Li atoms on atifluorite sites (black line in Fig. 6). The Li atoms at interstitial sites and those atoms to vacant sites are more shielded, thus giving the contributions between 3.8 and 2 ppm. The green and the orange lines in Fig 6 show these. The N atoms occupy fcc lattice sites, but most of them are coordinated with the Li interstitials, with Li-N distances between 2.4 Å and 2.6 Å, or have a vacancy in the first coordination shell, or both. The three features in the N spectrum sampled at 100 K are associated with these three different environments. Also the H spectrum shows an asymmetric tail at lower temperatures that can be attributed to the rigid orientation of the NH groups. However, the signature of the presence of defects is in this case less pronounced. All these features are smoothed out at higher temperature. In particular, the shoulder at 2.5 ppm of the Li spectrum disappears, due to the frequent hopping between interstitial and lattice sites and the longer residence-time in the antifluorite positions. Moreover, the diffusion of Li atoms induces some distortion in the N sublattice, and each N

experiences different local environments along the trajectory. The effect on the NMR spectrum is the broadening of the band that at 600 K covers a range more similar to the large signal distribution observed for the optimized (Fm-3d B) structure (see Fig 3).

## Conclusion

We presented an investigation of the lithium imide structure at low and high temperature, starting from structures that were previously proposed in the literature. The goal is to find possible fingerprints that can help in identifying the structure and the effects of Li mobility by experimental techniques, such as NMR spectroscopy. NMR spectroscopy is particularly suited for such a study because of its sensitivity to local environments, and it can provide valuable information also for substantially disordered systems.

Our characterization of the three optimized structures at 0K shows that structural parameters taking into account the long-range order and average structural properties, like pair distribution functions and X-Ray diffraction patterns, are not very useful to discriminate among the variations in the local environment induced by the formation of Frenkel pairs. Only the NMR spectra provide a clear identification. In particular, different Li chemical shifts could be associated to different types of interstitial environments. By considering the average shift obtained over the spectral profile, the agreement obtained from the optimized (Fm-3d A) structure with the available experimental data at 300 K is already quite good. On the contrary, the optimized structure of (Fm-3d B) produces spectra distributed over larger ranges. This seems to be less in agreement with the experiment. Our results confirm that the presence of Frenkel pairs stabilizes the structure also at 0K, in spite of the distortion of the N sublattice. At low temperature, below 400K, the MD simulations show first relaxation processes, involving a partial reorientation of the NH groups and hopping of some interstitial Li atoms into antifluorite sites. However, no proper Li mobility is observed. Only at higher temperature the hopping events involve also the Li atoms occupying antifuluorite sites. The resulting disorder in the Li sublattice, with dominant occupation of antifluorite sites, is the reason why $Li_2NH$ shows, at least on average, the

Fm-3m space group symmetry. The modification of the interstitials' distribution at lower temperature, as well as the set-up of diffusive behaviour at higher temperatures, are clearly captured by the calculation of the NMR chemical shift spectra. In particular, from the NMR chemical shift we are able to discriminate among different stable local environments. On the other hand, at higher temperature, these differences are smoothed out. The Li atoms start diffusing and experiencing all possible environments, thus leading to the order-disorder transition, as it was already observed previously.

In conclusion, the (Fd-3m A) structure, which was theoretically determined following the relaxation of the antifluorite at low temperature, is a good candidate as a low temperature structure of $Li_2NH$. It is consistent with the structural parameters of other defective structures, it provides the best agreement with the available experimental NMR data, and leads to the high temperature order-order transition already discussed by other authors.

ACKNOWLEDGMENT

The authors thank Dr. Guillermo Ludena for providing the structures, Dr. Valery Weber and Mr. Samuele Giani for helpful discussions on methodologies and simulation procedures concerning the calculation of NMR chemical shifts.

SUPPORTING INFORMATION PARAGRAPH

The supporting information contain details of our chemical shift calculations, including the statistical convergence of our NMR sampling (Figure S1). We have also added complementary cristallographic informations on our structure : the RMSD Li-Li distance (Figure S2) for the temperature from 100K to 900K, the PDB files at different temperature 100K, 300K and 600K (Figure S3 to S5), the X-Ray pattern and the distribution of the azimutal angle of the NH orientation at these three temperatures (Figure 6). This material is available free of charge via the Internet at http://pubs.acs.org.

FIGURE CAPTIONS

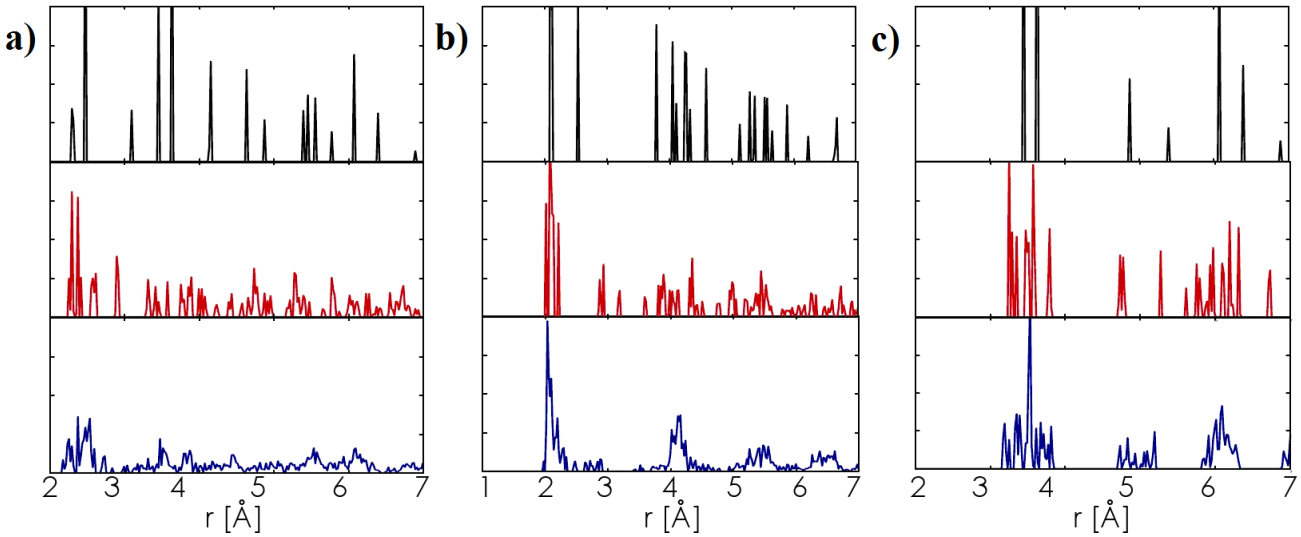


**Figure 1.** a, b, and c are the pair distribution functions Li-Li, Li-N, and N-N as computed from the three optimized structures for $Li_2NH$: Fm-3m (black), Fd-3m A (red), and Fd-3m B (blue).

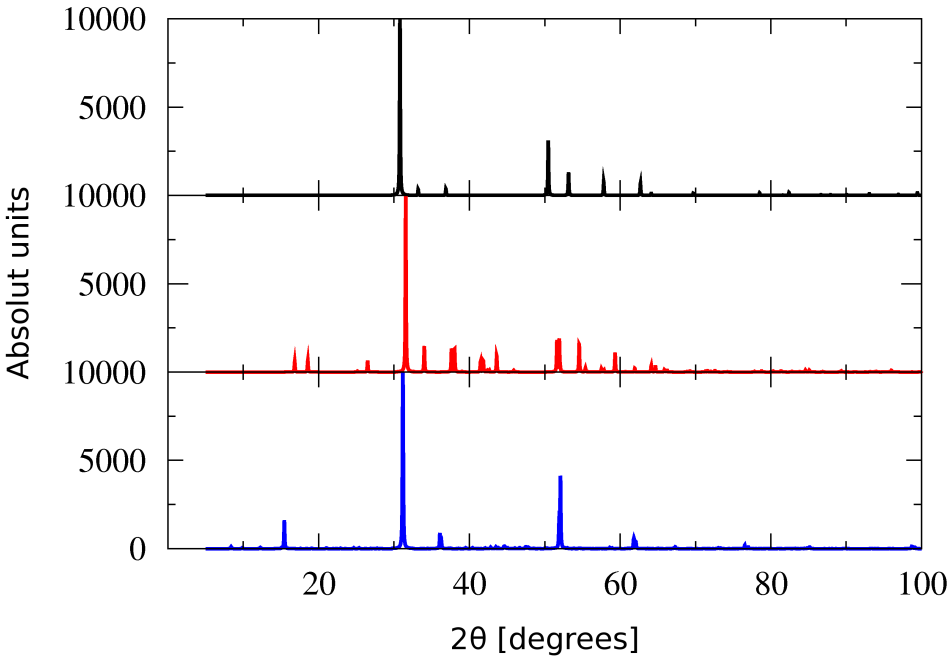


**Figure 2.** X-ray diffraction patterns computed on the three optimized $Li_2NH$ structures, i.e. Fm-3m (top), Fd-3m A(middle), Fd-3m B (bottom). The spectra are obtained with the software Mercury[22] using the parameter λ=1.54056 Å.

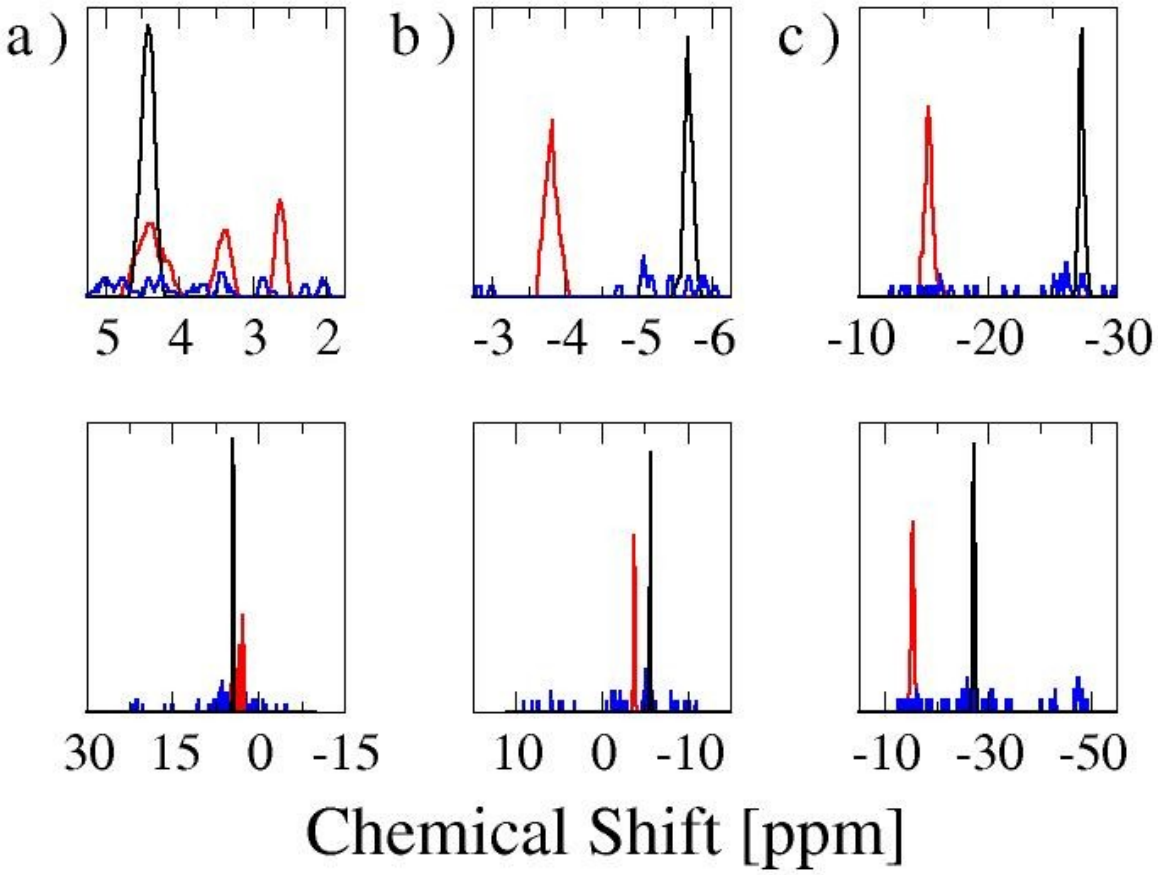


**Figure 3.** a) $^{7}$Li, b) $^{1}$H, and c) $^{15}$N NMR chemical shift spectra computed for the three $Li_2NH$ structures optimized at 0 K, i.e. Fm-3m (black), Fd-3m A (red), and Fd-3m B (blue). Notice that the plots in the top panels are zoom-in of the spectra reported in the bottom panel, where the full range obtained for Fd-3m B (blue) is reported.

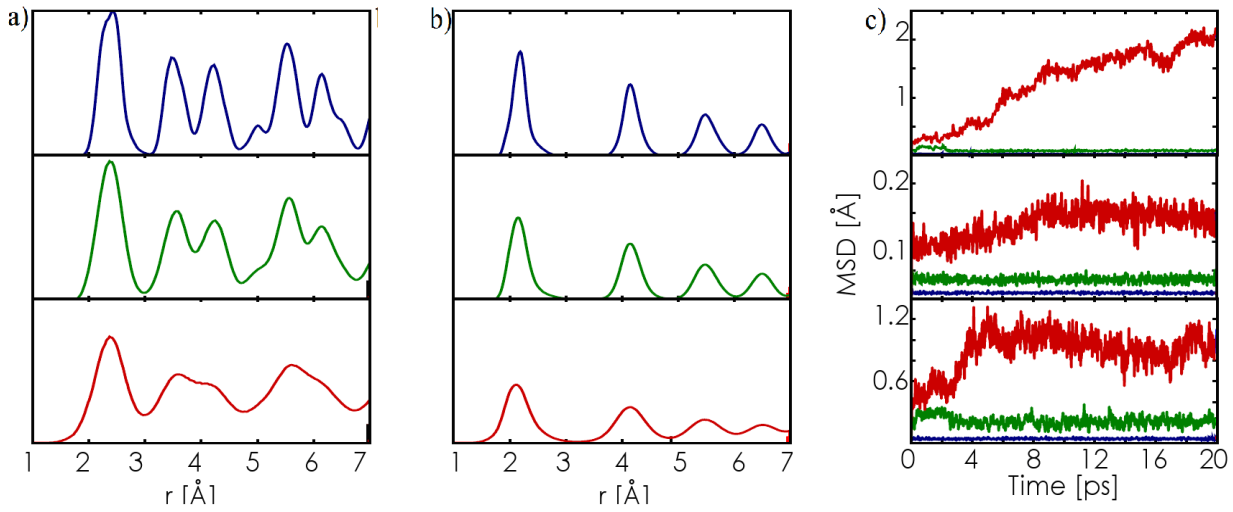


**Figure 4.** (a) and (b) Li-Li and the Li-N pair distribution functions, as averaged over the last 20 ps of the NVE trajectories generated at 100K (blue), 300K (green), and 600K (red). (c) Li (top panel), H (middle panel), and N (bottom panel) mean square displacement as monitored over the same NVE trajectories (same colour code as in (a) and (b)).

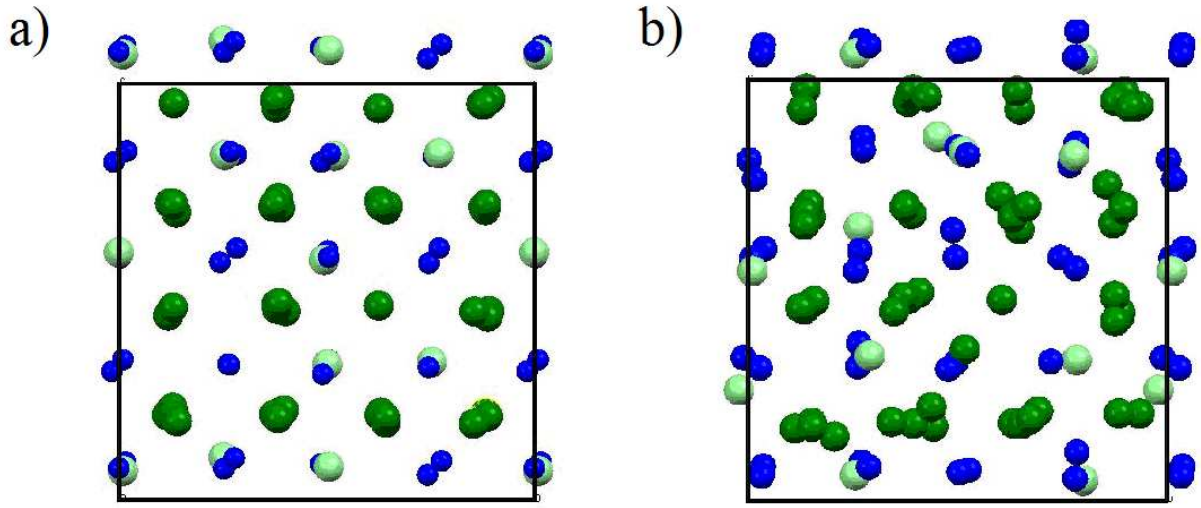


**Figure 5.** Li and N average positions of $Li_2NH$ as averaged over the last 20ps of the NVE trajectories generated at 100K (a), 600K (b). The blue spheres represent N atoms, the dark green spheres the Li atoms occupying antifluorite sites, and the light green spheres the Li interstitials.

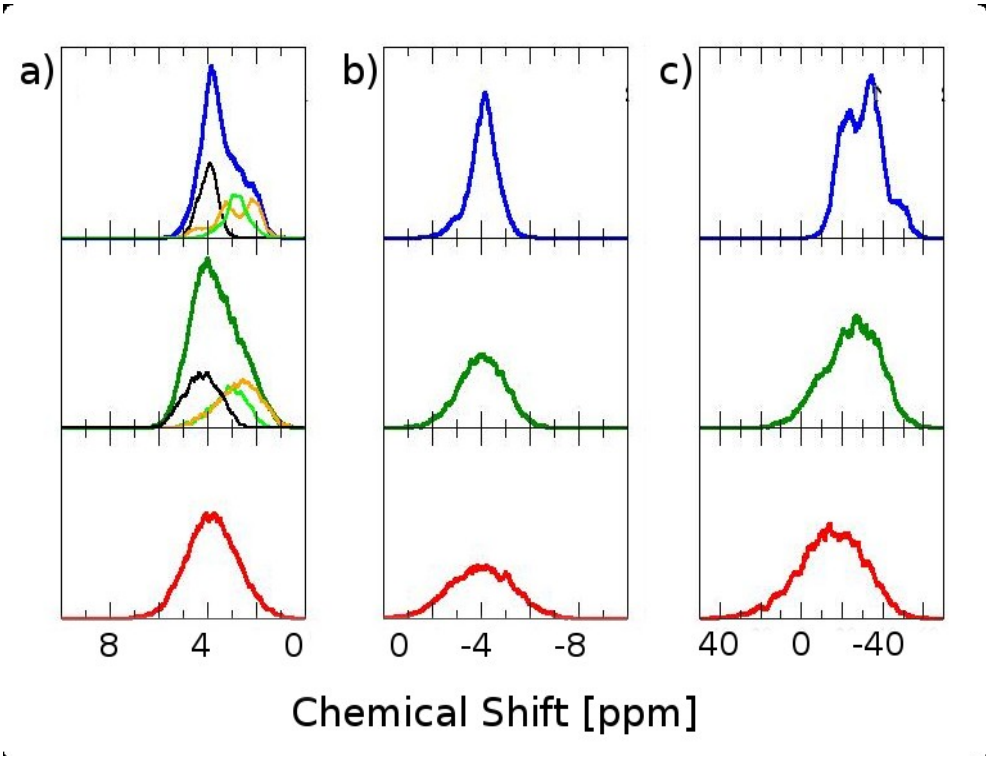


**Figure 6.** a) b) c) $^{7}$Li , $^{1}$H, and $^{15}$N NMR chemical shift spectra averaged over the last 20ps of the NVE trajectories generated at 100K (blue), 300K (dark green) and 600K (red) for our computed structure. At 100K and 300K the contributions of Li interstitials is given in light green, while in black and in orange are the contributions of Li atoms occupying lattice sites.

TABLES.

| Our Fd-3m | | | | |
|---|---|---|---|---|
| Lattice parameters a=10,014 | | | | |
| atomics Parameters | | | | |
| Atome | position | x | y | z |
| N | 16c, f=1 | 0+(Δ0,017) | 0+(Δ0,010) | 0+(Δ0,021) |
| | 16d, f=1 | 0,5+( Δ0,016) | 0.5+(Δ0,017) | 0.5+(Δ0.013) |
| H | 96g, f=1/3 | 0,04+(Δ0,013) | 0,04+( Δ+0,014) | 0,07+(Δ0,024) |
| Li | 8a f=1 | 0.125+( Δ+0,014) | 0.125+( Δ+0,010) | 0.125+( Δ+0,016) |
| | 8b f=1 | 0.375+( Δ+0,023) | 0.375+( Δ+0,010) | 0.375+( Δ+0,017) |
| | 48f f=37/48 | 0,375+ (Δ0,015) | 0,125+(Δ0,013) | 0,125+(Δ0,017) |
| | | | | |
| | 32e f=11/32 | 0,25+ (Δ0,018) | 0,25+(Δ0,015) | 0,25+(Δ0,020) |

Table 1 : Atomic positions describing the structure equilibrated at 300K by MD

| | $^{1}$H | | $^{7}$Li | |
|---|---|---|---|---|
| [ppm] | Exp. | MD | Exp. | MD |
| LiH | 2.7 | 2.2 (Δ=0.49) | 2.8 | 1.4 (Δ=0.61) |
| $Li_2NH$ | -4.7 | -4.2 (Δ=1.01) | 3.1 | 3.6 (Δ=1.05) |
| $LiNH_2$ | -2.2 | -1.6 (Δ=0.80) | 2.6 | 2.5 (Δ=0.58) |

**Table 2.** NMR average chemical shift at 300K (Exp. [Ref. 26] )

REFERENCES

[1] Schlapbach, L.; Zuttel, A. *Nature* **2001**, *414*, 353.

[2] a) Chen, P.; Xiong, Z. T.; Luo, J. Z.; Lin, J. Y.; Tan, K. L. *Nature* **2002**, *420*, 302; b) Chen, P.; Xiong, Z. T. ; Luo, J. Z.; Lin, J. Y.; Tan, K. L. *J. Phys. Chem. B* **2003**, *107*, 10967; c) Hu, Y. H.; Ruckenstein, E. *J. Phys. Chem. A* **2003**, *107*, 9737.

[3] a) Kar, T.; Scheiner, S.; Li, L. J. *J. Mol. Struct.:THEOCHEM* **2008**, *857*, 111; b) Kalinowski, J.; Berski, S.; Latajka, Z. *Chem. Phys. Lett.* **2011**, *501*, 587; c) Bonnet, M. L.; Tognetti, V. *Chem. Phys. Lett.* **2011**, *511*, 427.

[4] Forman, R. A. *J. Chem. Phys*. **1971**, *55*, 1987.

[5] a) Ohoyama, K.; Nakamori, Y.; Orimo, S.; Yamada, K. *J. Phys. Soc. Jpn.* **2005**, *74*, 483; b) Noritake, T.; Nozaki, H.; Aoki, M.; Towata, S.; Kitahara, G.; Nakamori, Y.; Orimo, S. *Alloys Compd.* **2005**, *393*, 264. c) Mueller, T.; Ceder, G. *Phys. Rev. B,* **2006**, *74*, 134104 Mueller, T.; Ceder, G. *Phys. Rev. B,* **2010**, *82*, 174307.

[6] Balogh, M. P.; Jones, C. Y. ; Herbst, J. F.; Hector Jr., L. G.; Kundrat, M. *J. Alloys Compd.* **2006**, *420*, 326.

[7] a) Herbst, J. F.; Hector, Jr., L. G. *Phys. Rev. B* **2005**, *72*, 125120; b) Hector, Jr., L.G.; Herbst, J. F. *J. Phys.: Condens. Matter* **2008**, *20*, 064229.

[8] Ludueña, G. A.; Wegner, M.; Bjalie, L.; Sebastiani, D.; *Chem. Phys. Chem*. **2010**, *11*, 2353.

[9] a) Miceli, G.; Cucinotta, C. S.; Bernasconi, M.; Parrinello, M. *J. Phys. Chem. C* **2010**, *114*, 15174; b) Miceli, G.; Ceriotti, M.; Bernasconi, M.; Parrinello, M. *Phys. Rev. B* **2011**, *83*, 054119.

[10] (05/02/2010) http://cp2k.berlios.de

[11] a) Hohenberg, P.; Kohn, W. *Phys. Rev.* **1964**, *136*, B864; b) Kohn, W.; Sham, L. J.; *Phys. Rev.* **1965**, *140,* A1133.

[12] a) Becke, A. D. *Phys. Rev. A* **1988**, *38*, 3098; b) Lee, C.; Yang, W.; Parr, R. G. *Phys. Rev. B* **1988**, *37*, 785.

[13] Goedeker, S.; Teter, M.; Hutter, J. *Phys. Rev. B* **1996**, *54*, 1703.

[14] VandeVondele, J.; Hutter, J. *J. Chem. Phys*. **2007**, *127*, 114105.

[15] Grimme, S. *J. Comput. Chem.* **2006**, *27*, 1787-1799.

[16] David, W. I. F.; Jones, M. O.; Gregory, D. H.; Jewell, C. M.; Johnson, S. R.; Walton, A.; Edwards, P. P. *J. Am. Chem. Soc.* **2007**, *129*, 1594.

[17] Jacobs, H.; Juza, R. *Anorg. Allg. Chem*. **1972**, *391*, 271.

[18] a) Krack, M.; Parrinello, M. *Phys. Chem. Chem. Phys*. **2000**, *2*, 2105; b) Iannuzzi, M.; Chassaing, T.; Wallman, T.; Hutter, J. *Chimia* **2005,** *59*, 499.

[19] Weber, V.; Iannuzzi, M.; Giani, S.; Hutter, J.; Declerck, R.; Waroqier, M. *J. Chem. Phys.* **2009**, *131*, 014106.

[20] Dunning, Jr., T. H. *J. Chem. Phys.* **1989**, *90*, 1007.

[21] Paier, J.; Diaconu, C. V.; Scuseria, G. E.; Guidon, M.; Vande Vondele, J.; Hutter, J. *Phys. Rev. B* **2009**, *80*, 174114.

[22] a) Marcrae, C. F.; Edgington, P. R.; McCabe, P.; Pidcock, E.; Shields, G. P.; Taylor, R.; Towler, M.; Van de Streek, J.; *J.Appl. Cryst.* **2006**, *39*, 453; b) Bruno, I. J.; Cole, J. C.; Edgington, P. R.; Kessler, M. K.; Macrae, C. F.; McCabe, P.; Pearson, J.; Taylor, R. *Acta Crystallogr.* **2002**, *B58*, 389; c) Taylor, R.; Macrae, C. F.; *Acta Cryst.* **2001**, *B57*, 815.

[23] Araújo, C. M.; Blomqvist, A.; Scheicher, R. H.; Chen, P.; Ahuja, R. *Phys. Rev. B* **2009**, *79*, 172101.

[24] Blomqvist, A.; Araujo, C. M.; Scheicher, R. H.; Srepusharawoot, P.; Li, W.; Chen, P.; Ahuja, R. *Phys. Rev. B* **2010**, *82*, 024304.

[25] Miceli, G.; Ceriotti, M.; Angioletti-Uberti, S.; Bernasconi, M.; Parrinello, M. *J. Phys. Chem. C* **2011**, *115*, 7076.

[26] a) Lu, C.; Hu, J. Z.; Kwak, J. H.; Yang, Z.; Ren, R.; Markmaitree, T.; Shaw, L. L.; *J. Power Sources* **2007**, *170*, 419; b) Hu, J. Z.; Kwak, J. H.; Yang, Z.; Osborn, W.; Matkmaitree, T.; Shaw, L. L. *J. Power Sources* **2008**, *181*, 116; c) Hu, J. Z.; Kwak, J. H.; Yang, Z.; Osborn, W.; Markmaitree, T.; Shaw. L. L. *J. Power Sources* **2008**, *182*, 278.

[27] Varin, R. A.; Jang, M.; Polanski, M.; *J. ALLOYS Compd.* **2010**, *491*, 658.

[28] Osborn, W.; Markmaitree, T.; Shaw, L. L.; Hu, J. Z.; Kwak, J.; Yang, Z. G. Int. J. H Ener. 2009, 34, 4331.

**Local Disorder in Lithium Imide:** The structural picture of Lithium Imide compounds is critically revised on the atomic scale. The local conformation of this system is crucial for understanding their microscopic hydrogen uptake and release processes. *Ab initio* molecular dynamique simulation and solid-state $^{1}H$, $^{7}Li$, $^{15}N$, NMR spectroscopy indicate local disorder of the lithium sublattice (see picture)

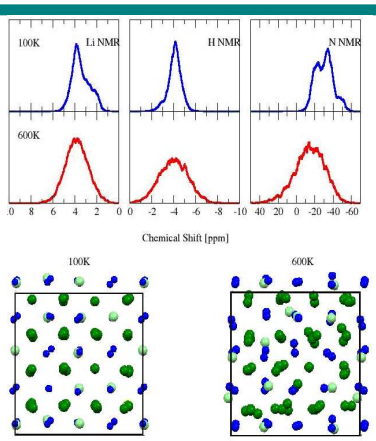


*M.-L. Bonnet, M. Iannuzzi*, D. Sebastiani, J. Hutter*

***Page No. – Page No.***

**Local Disorder in Lithium Imide from First principles simulation and NMR Spectroscopy**